EFSA では、段階的アプローチによる評価を推奨している。このアプローチでは、最初は、容易に入手可能なデータを用い、conservative な評価が行われ、結果として安全性が適切に保証されない場合には、より複雑で詳細な評価が行われる。ケーススタディとしてトリアゾール系農薬の複合暴露評価が行われたが、この段階的アプローチをルーチンベースで適用するには、特に CAG の設定や暴露評価に関していくつかの問題点があると結論された。最近、国際化学物質安全性計画 (IPCS)により公表された複合暴露評価のためのフレームワークは、EFSA と同様な階層的 (段階的)アプローチに基づいたものである。環境中には多くの化学物質が存在し、多くの化学物質が複合的に作用していると考えられる。リスク管理の優先度を決定するという意味でも、この階層的アプローチはより現実的で有効な手法と考えられる。

日本では、水道水中の農薬に関して、HIアプローチと類似した方法 (下記参照)による管理が行われている。

$$DI = \sum_{i=1}^{n} \frac{DV_i}{GV_i}$$

DI: 検出指標値 (1 を超えないこと)
DVi: 農薬 i の検出値
GVi: 農薬 i の目標値

HI 法は、用量相加性を仮定した conservative な手法であり、EFSA による複合リスク評価では最初の段階で実施された評価手法である。しかし、水質管理目標設定項目の対象外農薬であっても、飲料水以外の曝露経路 (食事等)を介して曝露される可能性があることや、極低濃度であっても、例えば有機リン系農薬のように 50 種もの物質が相加的に作用する可能性があることなどを考慮すると未だ十分な管理が行われているとはいえない可能性がある。米国 EPA では農薬以外にも消毒副生成物に関する複合リスク評価を行っており、日本の曝露状況下で、農薬や農薬以外の化学物質の複合リスクを評価する必要性や実施可能性について詳細な検討を行っていく必要がある。

2. パーフルオロ化合物の体内動態及び毒性に関する情報収集・整理

パーフルオロ化合物に関する最新の毒性関連情報を収集し整理した。その結果、特に PFOA 及び PFOS の肝毒性、発生毒性や免疫毒性に関する多くの研究成果の報告があった。また、これまでに全く報告がなかった PFOcDA 及び PFHxS の反復投与毒性や生殖発生毒性に関する新たな試験結果の報告があり、これまでは学会発表のみで詳細情報を入手することができなかった PFHxA の反復投与毒性及び生殖発生毒性試験や PFBS の 2 世代繁殖毒性試験のデータが専門誌で公表された。

PFBA、PFHxA、PFOA、PFOcDA、PFBS、PFHxS 及び PFOS に関しては、ラットに投与を行い広範な器官/組織への影響を調べた反復投与毒性試験の報告があり、いずれのパーフルオロ化合物についても、主な毒性ターゲットは肝臓であった。PFBA、PFHxA、PFHxS 及び PFOS については甲状腺、PFBS に関しては腎臓への影響も報告されている。パーフルオロ化合物の肝毒性ついては PPARα を介したメカニズムの関与が示唆されていたが、最近行われた PPARα 欠損マウスを用いた試験や遺伝子発現解析等の結果から、パーフルオロ化合物の肝毒性には PPARαに加え、CAR や PXR が関与していると考えられる。生殖発生毒性に関しては、PFBA、PFHxA、PFOA、PFNA、PFDeA、PFOcDA、PFBS、PFHxS 及び PFOS について、一世代/二世代試験、妊娠期投与試験や反復投与毒性・生殖発生毒性併合試験の結果が報告されており、最近は、PFOA による母動物及び児の乳腺への影響、PFOS による新生児死亡や神経発達影響に関する多くの研究成果の報告があった。PFBA、

PFOA、PFNA、PFDeA 及び PFOS については明確な母毒性がみられない用量で児の生存率及び体重の低下、生後発達や性成熟の遅れなどが認められた。PFOA、PFNA、PFDeA 及び PFOS については免疫毒性に関する報告があった。ラットで観察された影響は、体重増加抑制が引き起こされた、比較的高い用量での変化であり、二次的な変化の可能性が考えられる。一方、マウスでは、体重や血中のコルチゾール/コルチコステロンレベルに影響のみられない低用量で PFC 反応や T 細胞の増殖反応の低下等の影響が見られており、これらの変化の毒性学的な意義やヒトへの外挿性について検討する必要がある。

炭素鎖数が 4 及び 6 のパーフルオロ化合物と比較して、炭素鎖数 8～12 のパーフルオロ化合物の毒性は顕著に強かった。パーフルオロ化合物の血中排出半減期は炭素鎖の長さに依存して長くなる傾向が見られ、このことが炭素鎖が長いパーフルオロ化合物の方がより強い毒性を示す一つの要因と考えられている。一方、最近行われた PFOcDA の反復投与毒性・生殖発生毒性併合試験では、反復投与毒性及び生殖発生毒性に関する無毒性量は 40 mg/kg/day 及び 200 mg/kg/day と結論されており、炭素鎖数が 13～17 を超えると毒性は顕著に弱まると考えられる。炭素鎖数が 12 以上のパーフルオロ化合物の体内動態については全く情報が報告されていないことから、さらなる研究が望まれる。パーフルオロ化合物の体内動態には、明確な種差があり、霊長類における血中排出半減期はげっ歯類と比較して長かった。パーフルオロ化合物に職業的に暴露されたヒトを対象とした研究では、PFOA、PFHxS 及び PFOS の血清半減期はそれぞれ 3.8 年、8.5 年及び 5.4 年と顕著に長いことが報告されている。近年、疫学データ等のヒトを対象とした研究の成果が多く報告されており、これらの情報を収集及び整理した上で、ヒト健康へのリスクを適切に評価する必要があると考えられた。

パーフルオロ化合物は、紙・包装製品、カーペットや革・繊維製品の表面保護剤として、また、工業用界面活性剤、添加剤、コーティング剤や消火用泡等に広く使用されている。世界中の様々な地域の一般住民の血中から様々なパーフルオロ化合物が検出されていることから、これらの化合物への暴露による複合影響を評価する必要があるだろう。最近、毒性等価係数 (TEF)法のようなスケーリング補正によるパーフルオロ化合物の複合リスク評価の実施可能性が検討されているが、主として下記 4 つの理由から、現時点では、パーフルオロ化合物類に TEF アプローチを適用することは困難であると結論されている：(1) 単一の受容体を介して毒性が発現することを示す証拠がない、(2) それぞれのパーフルオロ化合物が及ぼす影響に質的な違いがある、(3) パーフルオロ化合物の影響が相加的であることを示すデータがない、(4) 広く使用されているパーフルオロ化合物について十分な毒性データがない。特に長鎖のパーフルオロ化合物については、曝露の可能性があるにもかかわらず、毒性データが全く得られていないものもあり、さらなる研究が望まれる。

3. 長鎖パーフルオロカルボン酸の毒性発現の違いに関する研究

炭素鎖の長さに依存して毒性が変化するパーフルオロカルボン酸類について、その毒性発現の違いの要因を明らかにすることを目的として、ラット血清中の PFCs の濃度を測定するための分析法を開発した。平成 24 年度に開発した分析法では、PFOcDA を投与していないラットの血清中からも PFOcDA が検出されたことから、今年度は、分析系内への PFCs 残存量を少なくするために、従来の LC よりも装置流路系の内容積が少なく、かつ高理論段数が得られる

UHPLC を用いた分析法を開発した。この方法を用いて、PFOcDA の反復投与毒性・生殖発生毒性試験のラット血清中の PFCs を再分析したところ、PFOcDA を投与していない対照群の血清中からはPFCsは検出されなかった。PFOcDA を投与したラットの血清試料中からは、PFOA, PFNA, PFDA などの PFOcDA 以外の PFCs が、PFOcDA よりも高い濃度で検出されたことから、これらの PFCs が毒性発現に寄与していると考えられる。投与に使用した PFOcDA 標準品の純度を調べた結果、PFOcDA の組成比は 99.2%と高かった。フッ素-炭素結合は非常に強固であることが知られており、長鎖パーフルオロカルボン酸類がβ酸化等により炭素数のより少ない化合物に代謝される可能性は低いと考えられる。吸収率及び排泄速度の違いにより、被験物質中に不純物として含まれていた微量の PFCs の存在比率が血中で顕著に増加した可能性が示唆された。

E. 結論

本年度は 3 つの研究を行った。1) 一昨年度から継続して行っている化学物質の複合暴露によるリスク評価手法に関する研究では、米国 EPA 及び EFSA で行われた農薬の複合リスク評価手法を調査し整理した。米国 EPA では、これまでに、RPF 法もしくはそれに準じた方法により、5 つの農薬グループの評価が行われており、いずれの農薬グループについても、健康影響の懸念はないと結論された。一方、EFSA では、段階的アプローチを推奨しており、ケーススタディとしてトリアゾール系農薬の複合リスク評価が行われた。最初に HI 法による評価が行われ、段階的により詳細で複雑な評価が繰り返し行われたが、結果として、この段階的アプローチをルーチンベースで適用するには、特に CAG の設定や暴露評価に関して問題点があると結論された。2) 環境を介した暴露によるヒトの健康への影響が懸念されるパーフルオロカルボン酸/スルホン酸類の毒性に関する最新情報を収集・整理した。その結果、2008 年以降、特に PFOA 及び PFOS の肝毒性、発生毒性や免疫毒性に関する多くの研究成果の報告があった。また、これまでに全く報告がなかった物質に関する試験結果の報告も認められた。しかし、PFOA 及び PFOS 以外の物質については毒性情報が未だ十分とは言えず、特に炭素数が 12 を超える長鎖のパーフルオロカルボン酸/スルホン酸類については、ほとんど情報は得られなかったことから、さらなる研究が望まれる。3) パーフルオロカルボン酸類の毒性強度が炭素鎖の長さに依存して変化する要因を明らかにすることを目的として、ラットの血清中 PFCs 濃度を測定するための分析法を開発した。平成 24 年度に開発した分析法を改良することにより、分析系内の PFCs 残存量を少なくすることができた。この方法を用いて、PFOcDA を投与したラットの血清中 PFCs を再分析したところ、PFOcDA 以外の PFCs が検出されたことから、これらの PFCs が毒性発現に関与している可能性が示唆された。

F. 研究発表

1. 論文発表

Fujitani, T., Ohyama, K., Hirose, A., Nishimura, T., Nakae, D. & Ogata, A. (2012): Teratogenicity of multi-wall carbon nanotube (MWCNT) in ICR mice. J Toxicol Sci **37,** 81-89.

Hasegawa, R., Hirata-Koizumi, M., Dourson, M.L., Parker, A., Ono, A. & Hirose, A. (2013): Safety assessment of boron by application of new uncertainty factors and their subdivision. Regul Toxicol Pharmacol **65,** 108-114.

Matsumoto, M., Serizawa, H., Sunaga, M., Kato, H., Takahashi, M., Hirata-Koizumi, M., Ono, A., Kamata, E. and Hirose, A. (2012) No toxicological effects on acute and repeated oral

gavage doses of single-wall or multi-wall carbon nanotube in rats. J Toxicol Sci 37, 463-474.

Ono, A., Takahashi, M., Hirose, A., Kamata, E., Kawamura, T., Yamazaki, T., Sato, K., Yamada, M., Fukumoto, T., Okamura, H., Mirokuji, Y. and Honma, M. (2012) Validation of the (Q)SAR combination approach for mutagenicity prediction of flavor chemicals. Food Chem Toxicol 50, 1538-1546.

Takahashi, M., Yabe, K., Kato, H., Kawamura, T., Matsumoto, M., Hirata-Koizumi, M., Ono, A. and Hirose, A. (2013) Reproductive and developmental toxicity screening test of 3-cyanopyridine in rats. Reprod Toxicol 35, 7-16.

Takahashi, M., Kato, H., Doi, Y., Hagiwara, A., Hirata-Koizumi, M., Ono, A., Kubota, R., Nishimura, T. and Hirose, A. (2012) Sub-acute oral toxicity study with fullerene C60 in rats. J Toxicol Sci 37, 353-361.

高橋美加, 松本真理子, 宮地繁樹, 菅野誠一郎, 菅谷芳雄, 平田睦子, 小野敦, 鎌田栄一, 広瀬明彦 (2012) OECD化学物質対策の動向（第19報）－第30回OECD高生産量化学物質初期評価会議（2010年パリ）. 化学生物総合管理 8, 47-53.

高橋美加, 松本真理子, 宮地繁樹, 菅野誠一郎, 菅谷芳雄, 平田睦子, 中嶋徳弥, 小野敦, 鎌田栄一, 広瀬明彦 (2012) OECD化学物質対策の動向（第21報）－第32回OECD高生産量化学物質初期評価会議（2011年パリ）. 化学生物総合管理 8, 166-172.

高橋美加, 松本真理子, 宮地繁樹, 菅野誠一郎, 菅谷芳雄, 平田睦子, 中嶋徳弥, 小野敦, 鎌田栄一, 広瀬明彦. (2012) OECD化学物質対策の動向（第20報）－第31回OECD高生産量化学物質初期評価会議（2010年オックスフォード）. 化学生物総合管理 8, 54-60.

平田睦子, 高橋美加, 松本真理子, 川村智子, 小野敦, 広瀬明彦 (2012) 小児用玩具に使用されるフタル酸エステル代替可塑剤の毒性影響. 国立医薬品食品衛生研究所報告第130号, 31-42.

松本真理子, 高橋美加, 平田睦子, 小野敦, 広瀬明彦. (2012) OECD高生産量化学物質点検プログラムからOECD化学物質共同評価プログラムへ, 化学物質総合管理 8, 173-233.

松本真理子, 宮地繁樹, 菅谷芳雄, 広瀬明彦 (2012) OECD高生産量化学物質点検プログラム：第31回初期評価会議概要. 化学生物総合管理 8, 28-36.

松本真理子, 宮地繁樹, 菅谷芳雄, 広瀬明彦. (2012) OECD高生産量化学物質点検プログラム：第32回初期評価会議概要. 化学生物総合管理 8, 37-46.

2.学会発表

Hirose, A., Takahashi, M., Kato, H., Doi, Y., Hagiwara, A., Hirata-Koizumi, M., Ono, A., Kubota, R. and Nishimura, T. (2012) Repeated dose toxicity of fullerene C60 by gavage for a month in rats. The 6th International Congress of Asian Society of Toxicology (2012.7) (Sendai, Japan).

Hirose, A., Ono, A., Hirata-Koizumi, M., Serizawa, H., Sunaga, M., Furukawa, M., Kamata, E. and Nishimura, T. (2012) Repeated dose 28-day oral toxicity studies of single- and multi-walled carbon nanotubes in rats. The 48th EUROTOX2012 (2012.6)(Sweden,Stockholm).

Ono, A., Ikeya, M., Suzuki, T., Nishimura, T., Kawamura, T., Takahashi, M., Matsumoto, M., Kato, H., Hirata-Koizumi, M., Hirose, A. (2012) A combined repeated dose and reproductive/developmental toxicity screening study of perfluoroundecanoic acid in rats. The

52nd SOT Annual meeting (2013.3) (San Antonio, TX, USA).

平田睦子, 藤井咲子, 古川正敏, 川村智子, 高橋美加, 松本真理子, 加藤日奈, 小野敦, 広瀬明彦. (2012) パーフルオロドデカン酸の反復経口投与毒性・生殖発生毒性併合試験. 第39回日本毒性学会学術年会（2012.7）（仙台）.

G. 知的財産

権の出願・登録状況（予定も含む）

1. 特許取得: 該当なし
2. 実用新案登録: 該当なし
3. その他: 該当なし

研究成果の刊行に関する一覧表

雑誌

発表者氏名	論文タイトル名	発表誌名	巻号	ページ	出版年
Quan D, Okashita R, Yanagibashi Y, Echigo S, Ohkouchi Y, Itoh S, Jinno H.	Exposure to Haloacetic Acids via Typical Components of the Japanese Diet and their Allocations of Drinking Water Ingestion to Total Exposure	J. Water Supply: Research and Technology-Aqua	in press		2013
Matsushita T, Suzuki H, Shirasaki N, Matsui Y, Ohno K.	Adsorptive virus removal with super-powdered activated carbon	Separation and Purification Technology	107	79–84	2013
Kimura M, Matsui Y, Kondo K, Ishikawa T.B, Matsushita T, Shirasaki N.	Minimizing residual aluminum concentration in treated water by tailoring properties of polyaluminum coagulants	Water Research	47(6)	2075-2084	2013
Jo I, Echigo S, Itoh S.	Profiles of dissolved organic matter and haloacetic acid formation potential in drinking water treatment by a comprehensive fractionation technique	Water Sci. Technol.	13(1)	89-94	2013
小坂浩司，黒田啓介，村上道夫，吉田伸江，浅見真理，小熊久美子，滝沢智，秋葉道宏	東京の地下水中の塩素酸イオンおよび過塩素酸イオンの実態調査	土木学会論文集G(環境)	69 (1)	10–18	2013
Matsui Y, Nakao S, Yoshida T, Taniguchi T, Matsushita T.	Natural organic matter that penetrates or does not penetrate activated carbon and competes or does not compete with geosmin	Separation and Purification Technology	113	75–82	2013
Matsui Y, Nakao S, Taniguchi T, Matsushita T.	Geosmin and 2-methylisoborneol removal using superfine powdered activated carbon: shell adsorption and branched-pore kinetic model analyse and optimal particle size	Water Research	47(8)	2873-2880	2013
Hasegawa R, Hirata-Koizumi M, Dourson M.L, Parker A, Ono A, Hirose A.	Safety assessment of boron by application of new uncertainty factors and their subdivision	Regul. Toxicol. Pharmacol.	65	108-114	2013

Takahashi M, Yabe K, Kato H, Kawamura T, Matsumoto M, Hirata-Koizumi M, Ono A, Hirose A.	Reproductive and developmental toxicity screening test of 3-cyanopyridine in rats	Reprod. Toxicol.	35	7-16	2013
白崎伸隆, 松下拓, 松井佳彦, 大芝淳	ウイルス処理に有効な新規アルミニウム系凝集剤の開発	土木学会論文集G(環境)	68(7)	III_41–50	2012
Shirasaki N, Matsushita T, Matsui Y, Urasaki T, Ohno K.	Difference in behaviors of F-specific DNA and RNA bacteriophages during coagulation-rapid sand filtration and coagulation-microfiltration processes	Water Science & Technology: Water Supply	12(5)	666–673	2012
Kishida N, Miyata R, Furuta A, Izumiyama S, Tsuneda S, Sekiguchi Y, Noda N, Akiba M.	Quantitative detection of Cryptosporidium oocyst in water source based on 18S rRNA by alternately binding probe competitive reverse transcription polymerase chain reaction (ABC-RT-PCR)	Water Research	46(1)	187-194	2012
Izumi T, Yagita K, Izumiyama S, Endo T, Itoh Y.	Depletion of Cryptosporidium parvum oocysts from contaminated sewage by using freshwater benthic pearl clams (Hyriopsis schlegeli)	Appl. Environ. Microbiol.	78(20)	7420-7428	2012
泉山信司, 遠藤卓郎	粉体ろ過によるクリプトスポリジウム濃縮保存法の開発	水道協会雑誌	81(9)	14–22	2012
黒木俊郎, 泉山信司, 八木田健司, 遠藤卓郎, 岸田直裕, 島崎大, 秋葉道宏	水道クリプトスポリジウム試験法の検査体制維持・向上に係る技術研修の役割	保健医療科学	Vol.61, No.5	454－463	2012
Kosaka K, Hayashida T, Terasaki M, Asami M, Yamada T, Itoh M, Akiba M.	Elution of bisphenol A and its chlorination by-products from lined pipes in water supply process	Water Science & Technology: Water Supply	12(6)	791-798	2012
Tani K, Matsui Y, Iwao K, Kamata M, Matsushita T.	Selecting analytical target pesticides in monitoring: sensitivity analysis and scoring	Water Research	46(3)	741–749	2012
Hirata-Koizumi M, Fujii S, Furukawa M, Ono A, Hirose A.	Repeated dose and reproductive/developmental toxicity of perfluorooctadecanoic acid in rats	J. Toxicol. Sci.	37	63-79	2012
Luilo G., Kosaka K, Asami M.	Chlorine demands of amino acids and amino sugars in water	J. Water Environ. Technol.	10 (2)	141–154	2012
Matsui Y, Yoshida T, Nakao S, Knappe DRU, Matsushita T.	Characteristics of competitive adsorption between 2-methylisoborneol and natural organic matter on superfine and conventionally sized powdered activated carbons	Water Research	46	4741-4749	2012

田原麻衣子，中島晋也，杉本直樹，有薗幸司，西村哲治	水道水質試験の標準液調製における不確かさと定量精度に影響を及ぼす要因	水道協会雑誌	81(5)	10-16	2012
Fujitani T, Ohyama K, Hirose A, Nishimura T, Nakae D, Ogata A.	Teratogenicity of multi-wall carbon nanotube (MWCNT) in ICR mice	J. Toxicol. Sci.	37	81-89	2012
Matsumoto M, Serizawa H, Sunaga M, Kato H, Takahashi M, Hirata-Koizumi M, Ono A, Kamata E, Hirose A.	No toxicological effects on acute and repeated oral gavage doses of single-wall or multi-wall carbon nanotube in rats	J Toxicol Sci.	37	463-474	2012
Ono A, Takahashi M, Hirose A, Kamata E, Kawamura T, Yamazaki T, Sato K, Yamada M, Fukumoto T, Okamura H, Mirokuji Y, Honma M.	Validation of the (Q)SAR combination approach for mutagenicity prediction of flavor chemicals	Food Chem. Toxicol.	50	1538-1546	2012
Takahashi M, Kato H, Doi Y, Hagiwara A, Hirata-Koizumi M, Ono A, Kubota R, Nishimura T, Hirose A.	Sub-acute oral toxicity study with fullerene C60 in rats	J. Toxicol. Sci.	37	353-361	2012
高橋美加，松本真理子，宮地繁樹，菅野誠一郎，菅谷芳雄，平田睦子，小野敦，鎌田栄一，広瀬明彦	OECD化学物質対策の動向（第19報）－第30回OECD高生産量化学物質初期評価会議（2010年パリ）	化学生物総合管理	8	47-53	2012
高橋美加，松本真理子，宮地繁樹，菅野誠一郎，菅谷芳雄，平田睦子，中嶋徳弥，小野敦，鎌田栄一，広瀬明彦	OECD化学物質対策の動向（第21報）－第32回OECD高生産量化学物質初期評価会議（2011年パリ）	化学生物総合管理	8	166-172	2012
高橋美加，松本真理子，宮地繁樹，菅野誠一郎，菅谷芳雄，平田睦子，中嶋徳弥，小野敦，鎌田栄一，広瀬明彦	OECD化学物質対策の動向（第20報）－第31回OECD高生産量化学物質初期評価会議（2010年オックスフォード）	化学生物総合管理	8	54-60	2012
平田睦子，高橋美加，松本真理子，川村智子，小野敦，広瀬明彦	小児用玩具に使用されるフタル酸エステル代替可塑剤の毒性影響	国立医薬品食品衛生研究所報告	第130号	31-42	2012

松本真理子, 高橋美加, 平田睦子, 小野敦, 広瀬明彦	OECD高生産量化学物質点検プログラムからOECD化学物質共同評価プログラムへ	化学物質総合管理	8	173-233	2012
松本真理子, 宮地繁樹, 菅谷芳雄, 広瀬明彦	OECD高生産量化学物質点検プログラム：第31回初期評価会議概要	化学生物総合管理	8	28-36	2012
松本真理子, 宮地繁樹, 菅谷芳雄, 広瀬明彦	OECD高生産量化学物質点検プログラム：第32回初期評価会議概要	化学生物総合管理	8	37-46	2012

研究成果の刊行物・別刷

Separation and Purification Technology 107 (2013) 79–84

Contents lists available at SciVerse ScienceDirect

Separation and Purification Technology

journal homepage: www.elsevier.com/locate/seppur

Adsorptive virus removal with super-powdered activated carbon

Taku Matsushita *, Hideaki Suzuki, Nobutaka Shirasaki, Yoshihiko Matsui, Koichi Ohno

Graduate School of Engineering, Hokkaido University, N13W8, Sapporo 060-8628, Japan

ARTICLE INFO

Article history:
Received 17 April 2012
Received in revised form 10 January 2013
Accepted 15 January 2013
Available online 31 January 2013

Keywords:
Bacteriophage
Drinking water treatment
Hydrophobicity
Zeta potential

ABSTRACT

We investigated the removal of bacteriophages by adsorption on commercially available powdered activated carbon (N-PAC, median diameter >10 μm) and super-powdered activated carbon (S-PAC, median diameter 0.7–2.8 μm). N-PACs failed to remove the virus in Milli-Q water buffered with 100 μM Ca^{2+}, but some S-PACs successfully removed it under the same condition. Three factors contributed substantially to virus removal: a smaller electrophoretic repulsive force between the virus and the PAC particles, a large proportion of pores 20–50 nm in diameter, and a greater hydrophobicity of the virus surface.

1. Introduction

The development of detection techniques based on molecular biology has enabled us to detect fragments of viral genomes in environmental waters, including drinking water sources, highlighting the need to ensure the removal of viruses at drinking water treatment plants. Although disinfecting water with hypochlorite ensures the biological safety of the finished water, the risk of virus infections can be reduced by physicochemical treatments such as coagulation–sedimentation–sand filtration; physical sieving processes such as ultrafiltration, nanofiltration, and reverse osmosis; and ozonation and UV irradiation.

Activated carbon adsorption is widely used to treat drinking water in Japan. Granular activated carbon (GAC) is used in combination with ozonation for removing byproducts derived from the oxidative decomposition of organic matter. Powdered activated carbon (PAC) is seasonally applied with excellent results for removing chemicals with an earthy–musty odor and pesticides. It has also been tested for virus removal. Adsorption experiments with a GAC-loaded (20 × 50 mesh, equivalent to 297–853 μm) column-type reactor removed only 24–50% of poliovirus [1]. Worse, GAC filtration did not remove bacteriophage MS2 [2]. These results indicate that GAC is not suitable for substantial virus removal within the contact time allowed in actual drinking water treatment, probably on account of a low rate of adsorption of virus. Indeed, only 70% of bacteriophage T4 was removed by activated carbon (300–425 μm) after 2 h of contact time [3]. Accordingly, effective virus removal by activated carbon will require a longer contact time, an extremely high dose of activated carbon, or both.

Reducing the particle size of activated carbon increases the rate of adsorption [4,5], because the travel distance for intraparticle radial diffusion is reduced and the specific surface area per adsorbent mass is increased [6]. Pulverizing activated carbon would therefore overcome the problems of slow adsorption kinetics, but the PAC particle size was previously limited to about 5 μm. Recent advances in nanotechnology now enable pulverization down to submicron or nanometer size ranges at a reasonable cost, producing super-powdered activated carbon (S-PAC) [7–9]. As S-PAC might improve virus removal, our objectives were to investigate the effect of pulverization of PAC particles on virus removal and the factors contributing to virus removal.

2. Materials and methods

2.1. Activated carbon

We tested 11 commercially available, thermally activated, normal PACs (N-PACs): 9 wood-based, 2 coconut-based, and 1 coal-based (Table 1). To prepare the S-PACs, we ground the N-PACs in a wet bead mill (Metawater Co., Ltd., Tokyo, Japan). We used both sets of materials to determine the effects of particle size on virus removal by adsorption. The PACs were dried in an oven at 105 °C and stored in a desiccator before use. They were then made into 5% slurries in Milli-Q water (Milli-Q Advantage, Millipore Corp., Billerica, MA, USA) and placed under vacuum to remove any air from the pores. The slurries were stored at 4 °C before dilution for use in the experiments. The particle size distributions were determined by laser scattering (LMS-30 Micron Sizer; Seishin Enterprise Co., Ltd., Tokyo, Japan). The surfaces of the N-PACs were observed by scanning transmission electron microscopy (SEM, JSM-7400F; JEOL Ltd., Tokyo, Japan).

* Corresponding author. Tel./fax: +81 11 706 7279.
E-mail address: taku-m@eng.hokudai.ac.jp (T. Matsushita).

1383-5866/$ - see front matter © 2013 Published by Elsevier B.V.
http://dx.doi.org/10.1016/j.seppur.2013.01.017

Table 1
Activated carbon used.

	Raw material	Median diameter (μm)		Key characteristics of S-PAC						
				Specific surface area[a] (m^2/g)	Element contents[b] (%)				Functional group[c]	
		S-PAC	N-PAC		C	O	N	S	Acidic	Basic
Wood-1	Wood	0.69	13.24	1145 ± 33	85.3 ± 0.6	7.05 ± 0.97	0.14 ± 0.01	0.10 ± 0.02	350 ± 9	790 ± 21
Wood-2	Wood	0.83	4.5	873 ± 39	80.0 ± 1.5	6.70 ± 0.51	0.25 ± 0.02	0.20 ± 0.02	193 ± 58	711 ± 139
Wood-3	Wood	1.49	NA	NA	NA	NA	NA	NA	NA	NA
Wood-4	Wood	0.66	NA	NA	84.6 ± 0.8	6.72 ± 0.11	0.15 ± 0.00	0.11 ± 0.03	NA	NA
Wood-5	Wood	2.79	NA	NA	NA	NA	NA	NA	NA	NA
Wood-6	Wood	1.38	NA	NA	NA	NA	NA	NA	NA	NA
Wood-7	Wood	2.20	NA	NA	NA	NA	NA	NA	NA	NA
Wood-8	Wood	0.93	11.46	1174 ± 14	81.9 ± 0.6	8.24 ± 0.48	0.20 ± 0.01	0.15 ± 0.02	351 ± 22	780 ± 56
Wood-9	Wood	1.65	0.6	NA	NA	NA	NA	NA	NA	NA
Coconut-1	Coconut shell	0.67	NA	NA	88.1 ± 0.5	5.95 ± 0.41	0.16 ± 0.02	0.11 ± 0.03	425 ± 34	329 ± 35
Coconut-2	Coconut shell	0.65	19.13	1215 ± 149	89.1 ± 0.2	5.30 ± 0.10	0.18 ± 0.04	0.06 ± 0.02	433 ± 16	582 ± 29
Coal-1	Coal	0.67	NA	NA	79.2 ± 0.3	10.62 ± 0.24	0.38 ± 0.00	0.55 ± 0.01	757 ± 36	366 ± 36
Determination coefficient (r^2) between logarithmic virus removal indicated in Fig. 2				0.38	0.01	0.06	0.06	0.06	0.08	0.10

NA – not applicable.
[a] Determined with BET.
[b] Measured with an elemental analyzer (Vario EL III, Elementar Analysensysteme GmbH, Hanau, Germany).
[c] Measured with Boehm titration [28,29].

2.2. Viruses

As model viruses we used two bacteriophages, Qβ (NBRC 20012) and MS2 (NBRC 20015), obtained from the Biological Resource Center (NBRC) of the National Institute of Technology and Evaluation (Chiba, Japan). The diameters of Qβ and MS2 are 23.5 ± 0.8 nm and 22.5 ± 1.0 nm, respectively [10]. The viruses were propagated for 22–24 h at 37 °C in *Escherichia coli* F^+ (NBRC 13965) obtained from NBRC. The cultures were centrifuged at 3000*g* for 10 min and then filtered through a 0.45-μm pore-size membrane (cellulose acetate; DISMIC-25cs; Toyo Roshi Kaisya, Ltd., Tokyo, Japan). The filtrate was purified twice in a centrifugal filter device (molecular weight cutoff: 100,000; Centriplus-100; Millipore Corp., Billerica, MA, USA) to prepare virus stock solution. Virus concentrations were measured by the plaque-forming unit (PFU) method according to the agar overlay method [11] using the bacterial host *E. coli* F^+. Average plaque counts of triplicate plates prepared from one sample gave the virus concentration.

2.3. Batch adsorption test

Milli-Q water was buffered with 424 μM $NaHCO_3$ to give the equivalent of 20 mg-$CaCO_3$/L of alkalinity (buffered Milli-Q water). The buffered Milli-Q water was supplemented with 0, 100, 200, 300, 400, or 500 μM $CaCl_2$. In a square beaker, 500 mL of solution was adjusted to pH 6.8 with HCl, and either Qβ or MS2 was added to give 10^6 PFU/mL. PAC was added at 20 mg/L and the suspension was continuously stirred at $G = 200\ s^{-1}$ with a jar tester. Samples were withdrawn at 0, 1, 2, 4, and 8 h and filtered through a membrane ($\phi = 0.2$ μm, PTFE; Toyo Roshi Kaisya) to remove the PAC particles. The virus concentration in the permeate was measured by the PFU method.

2.4. Electrophoretic mobility

All solutions were held for 1 day at 20 °C for the pH to stabilize. Just before measurement, each S-PAC or virus was suspended in the solution at ~20 mg/L or 10^9 PFU/mL, respectively. The electrophoretic mobility of S-PACs and viruses was measured with an electrophoretic light-scattering spectrophotometer (Zetasizer Nano ZS, 532 nm green laser; Malvern Instruments Ltd., Malvern, Worcestershire, UK) at 25 °C and at a 17° measurement angle.

2.5. Pore size distribution analyses of PACs

Pore size was analyzed by nitrogen gas adsorption at 77 K with an automated gas sorption analyzer (Autosorb-iQ-MP; Quantachrome Instruments, Boynton Beach, FL, USA). Pore size distributions were determined by a combination of two widely accepted models: the DFT model for the pore size distribution of micropores (<2 nm) and the BJH theory for the volumes of mesopores and macropores (>2 nm).

2.6. Virus hydrophobicity

Hydrophobicity was estimated by the bacterial adhesion to hydrocarbon (BATH) method [12]. Virus was added to 3 mL of buffered Milli-Q water at a final concentration of ~10^8 PFU/mL at pH 7.0. The solution was supplemented with 0.25 mL of solvent (*n*-hexadecane, *n*-octane, or *p*-xylene). The solution was intensely vortexed for 2 min, and then rested for 15 min at room temperature to allow the solvent and water to separate. The virus concentration in the water phase was measured by real-time PCR [13]. A decrease in virus concentration was used as a measure of the virus surface hydrophobicity [12].

3. Results and discussion

3.1. Comparison of virus removal between N-PACs and S-PACs

Virus removal increased with time even without PAC dosing (black circles), probably owing to spontaneous inactivation (Fig. 1). N-PACs (white circles) of wood-8 and coconut-2 showed the same result as the control. S-PACs of wood-8 and coconut-2 (gray circles) also showed the same result, even though their outer surface areas per unit mass were 12.3× and 29.4× those of the N-PACs, respectively. N-PAC of wood-1 removed some virus. In contrast, S-PAC of wood-1, with 19.2× the outer surface area of the N-PAC, caused a monotonic decrease in virus concentration with contact time, reaching a 4 log reduction after 8 h. Our result appears to disagree with that of Powell et al. [14], who reported

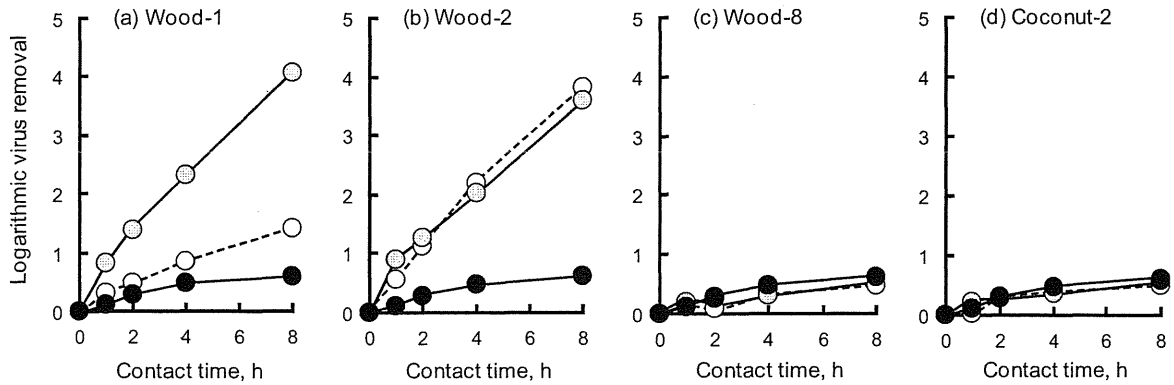

Fig. 1. Changes in virus (Qβ) removal with contact time (Ca^{2+} = 100 μM). Gray, white and black circles indicate SPAC, N-PAC and control, respectively.

that the adsorption of bacteriophage MS2 to a GAC reached equilibrium in 3 h. However, whereas they found that the amount of virus *adsorbed* had plateaued (>99% removal), we monitored the concentration of virus in the *liquid phase*, which might have decreased further even after 99% of the virus was adsorbed. N-PAC of wood-2 removed virus at the same extent as S-PAC of wood-1, possibly because the particle size of N-PAC of wood-2 was much smaller than those of other N-PACs. Virus removal with S-PAC of wood-2 was almost the same to that with the N-PAC, possibly because the N-PAC was small enough to remove the virus and its outer surface area was not so much increased with the pulverization (5.4×). The pulverization enhanced the adsorptive removal by the wood-1 PAC, but not by the wood-2, wood-8 and coconut-2 PACs. Overall, the effect of pulverization on virus removal might depend on the intrinsic characteristics of the PACs.

3.2. Effects of median diameter and PAC source on virus removal

We expected that finer PACs would remove more virus. However, different S-PACs with the same median diameter of ~0.7 μm showed very different removals of virus: wood-1 and wood-2 S-PACs achieved a removal of ~4 orders of magnitude (4 logs), whereas the other S-PACs achieved a removal of <2 logs (Fig. 2). Virus removal may be influenced by many factors such as raw material, specific surface area, element content, surface functional group, pore size distribution and surface charge. Nevertheless, as the capacity of the wood-based PACs varied widely from 0.5 to 4 logs, and a coconut-based PAC removed more virus than some wood-based PACs, the difference in virus removal seems to be due to more than the raw materials. The inherent characteristics of PAC listed in Table 1, i.e. specific surface area, element content and surface functional group, obviously had no relationship with the virus removal ($r^2 < 0.4$); other inherent factors most likely had influence on the adsorptive removal. To investigate the factors affecting the removal, we made a comparison in the following sections among two S-PACs that exhibited the highest virus removal (i.e. wood-1 and wood-2 S-PACs) and 2 S-PACs that had similar particle diameters to the superior S-PACs but exhibited the lowest virus removal (i.e. wood-8 and coconut-2 S-PACs).

3.3. Effect of surface charge of PACs on virus removal

When virus and S-PACs were dispersed in buffered Milli-Q water without Ca^{2+}, both particles were highly negatively charged, and the electrostatic repulsive force between them, measured as electrophoretic mobility, was high (Fig. 3). As the Ca^{2+} concentra-

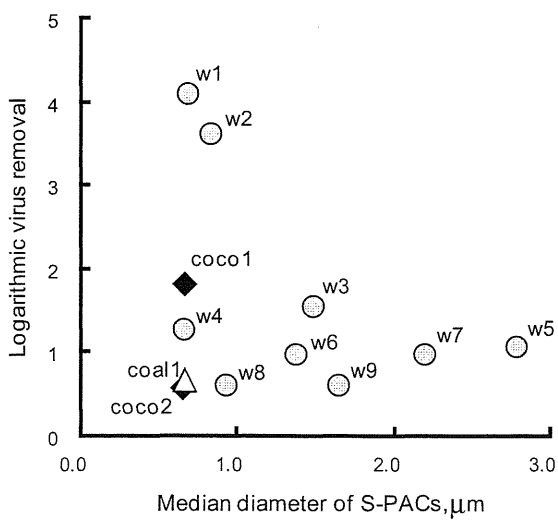

Fig. 2. Relationship between median diameter of S-PACs and virus removal (contact time = 8 h, Ca^{2+} = 100 μM). Circles, diamonds and triangle represent wood-, coconut- and coal-based SPACs. Logarithmic virus removals for wood-1, wood-2, wood-8 and coconut-2 S-PACs were averaged values of two experiments with too small deviations to see, while those for other S-PACs were obtained in one experiment.

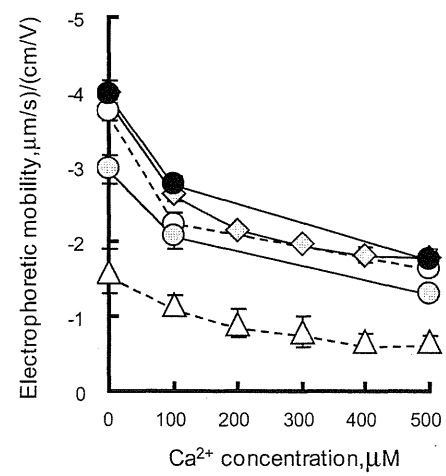

Fig. 3. Electrophoretic mobility of Qβ and S-PACs at different concentrations of Ca^{2+}. White, gray and black circles, gray diamonds and white triangles indicate wood-1, wood-2, wood-8, coconut-2 and Qβ, respectively. Error bars indicate SD of 10 measurements.

tion increased, the electrophoretic mobilities of both virus and S-PACs decreased. In general, an increase in ionic strength compresses the diffuse layer of ions surrounding a charged particle, decreasing the extent of the charge. This behavior has been seen before in viruses [15–18]. Our results support this.

The repulsion energy (V_R) of the electrical double layer between two closely spaced spheres is described as follows [19]:

$$V_R = 2\pi\varepsilon\zeta_1\zeta_2\frac{d_1 d_2}{d_1 + d_2}\exp(-\kappa h) \quad (1)$$

where ε is the permittivity of the medium, ζ_1 and ζ_2 are the zeta potentials of the spheres, d_1 and d_2 are the diameters of the spheres, and h is the minimum surface-to-surface separation between the spheres. κ is the Debye–Hückel reciprocal length:

$$\kappa = \sqrt{\frac{e^2\sum n_{i0}z_i^2}{\varepsilon kT}} \quad (2)$$

where e is the elementary charge, n_0 is the number concentration of ions in the bulk solution, z is the valency of the ion, k is the Boltzmann constant, and T is the absolute temperature. When virus and S-PAC were spaced 0.2 nm apart, as the Ca^{2+} concentration increased, the repulsion decreased (Fig. 4). Virus removal improved from 1–3 logs at 0 μM-Ca^{2+} to 3–6 logs at 500 μM-Ca^{2+}. Thus, virus removal was enhanced as the repulsion decreased. A higher ionic strength compresses the electrical double-layer of charged particles, reducing the electrostatic repulsion between like-charged particles and enabling the particles to move nearer to each other [17,21,22]. The adsorption of the virus onto the S-PAC was most likely hampered by the electrostatic repulsive force between them. Therefore, reducing the repulsion by increasing the ionic strength improved virus removal. One explanation is that the positive ions shield the negative charges on the surfaces of the adsorbate and the adsorbent, decreasing the net electrostatic repulsion between the particles [16,18,20,23]. Or Ca^{2+} may electrically adsorb to a negatively charged moiety of both adsorbate and adsorbent concurrently, forming a cation bridge to link the like-charged particles [18,23,24].

Fig. 5 shows the relationship between the virus removal and the electrical double layer repulsion energy. Virus removal tended to increase as the repulsive force decreased, but the removal performances were different among s-PACs. Wood-1 S-PAC exhibited superior virus removal across all repulsion energy range: the virus removal with wood-1 S-PAC was always greater than those with other S-PACs tested even in the range in which the repulsive force

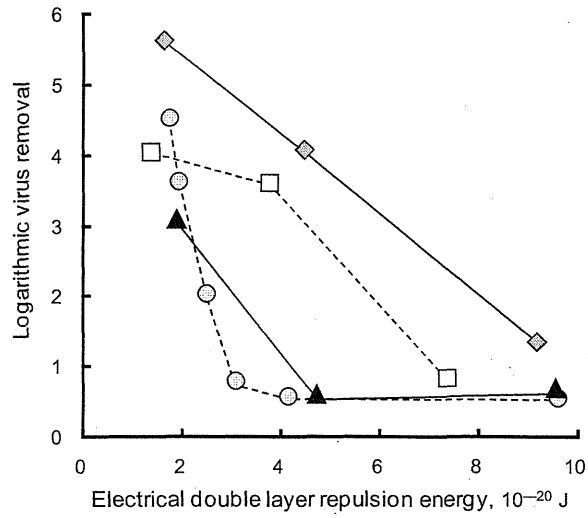

Fig. 5. Relationship between virus removal (Qβ, contact time = 8 h) and repulsion energy of electrical double layer (0.2 nm distance). Gray diamonds, white squares, black triangles and gray circles indicate wood-1, 2, 8 and coconut-2, respectively. Repulsion energy was controlled by Ca^{2+} concentration.

working between the virus and S-PAC particles was the same. These observations mean that the electrostatic repulsion can explain the extent of virus removal by each S-PAC under different ionic conditions, but not the difference between different types of PAC.

The logarithmic virus removals of wood-1 and wood-2 S-PACs linearly increased with decrease in the electrical double layer repulsion energy. In contrast, the virus removals of wood-8 and coconut-2 S-PACs did not change even when the repulsion energy decreased down from 10×10^{-20} to 3×10^{-20} J, but seem to increase drastically when the repulsion energy was smaller than 3×10^{-20} J. Possible reason for this observation is discussed in the following section.

3.4. Effect of pore size distribution of PACs on virus removal

SEM observations revealed that the wood-1 and wood-2 S-PACs, which could remove virus effectively, had a rough surface with many mesopores 20–50 nm in diameter (Photo 1). In contrast,

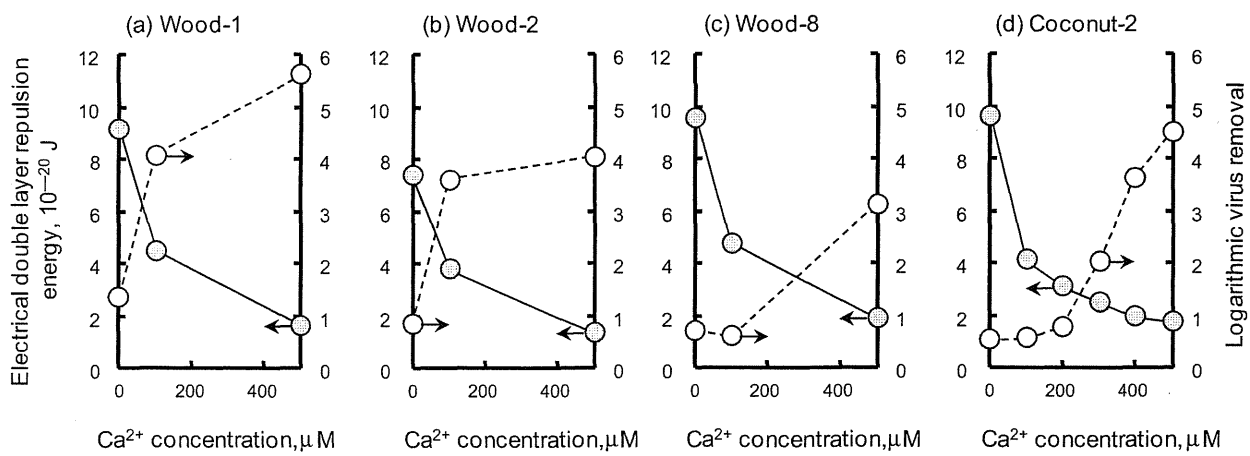

Fig. 4. Changes in repulsion energy of electrical double layer between the virus and S-PACs at 0.2 nm distance, and virus removal (Qβ, contact time = 8 h) with increase in Ca^{2+} concentration. Gray and white circles indicate the electrical double layer repulsion energy and the logarithmic virus removal, respectively.

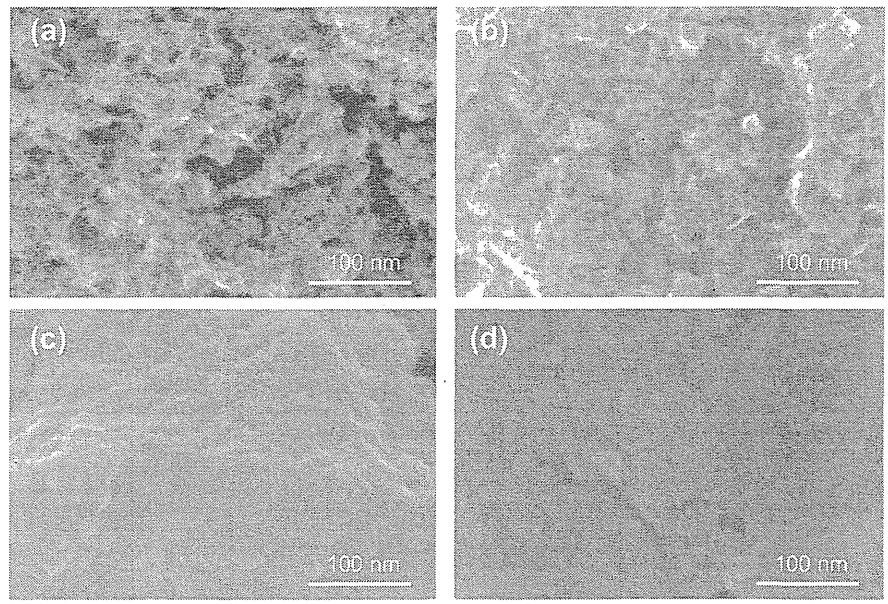

Photo 1. SEM images of S-PAC surfaces: (a) wood-1; (b) wood-2; (c) wood-8; and (d) coconut-2.

Table 2
Comparison in pore volume among S-PACs.

Pore diameter (nm)	Wood-1	Wood-2	Wood-8	Coconut-2
1–2	0.203	0.123	0.206	0.177
2–3	0.040	0.040	0.056	0.030
3–5	0.071	0.091	0.053	0.044
5–10	0.063	0.088	0.038	0.037
10–20	0.044	0.066	0.025	0.028
20–50	0.035	0.039	0.017	0.022

Table 3
Logarithmic removals of Qβ and MS2 with S-PACs (contact time = 8 h, Ca^{2+} = 100 μM).

	Wood-1	Wood-2
Qβ	4.1	3.6
MS2	3.0	2.9

the wood-8 and coconut-2 S-PACs, whose virus removal was poor, had a relatively smooth surface with no mesopores. With a diameter of ~23 nm, the virus cannot pass through pores smaller than this. The nearer the diameter of an adsorbate molecule is to the pore size of an adsorbent, the greater is the attraction [25]. Therefore, the wood-1 and wood-2 S-PACs, with pores 20–50 nm wide, offered good conditions for the virus to settle in, and so removed it effectively. This most likely contributed to the difference of behaviors of viruses in the relationship between the logarithmic virus removal and the electrical double layer repulsion energy indicated in Fig. 5: the wood-1 and wood-2 could easily capture the virus particles with many suitable pores for the virus particles to settle in even under the large repulsion energy that prevented the adsorption of the virus particles to the wood-8 and coconut-2 S-PACs. At this moment, the reason why the virus removals of wood-8 and coconut-2 S-PACs increased drastically with the decrease in the repulsion energy is not clear.

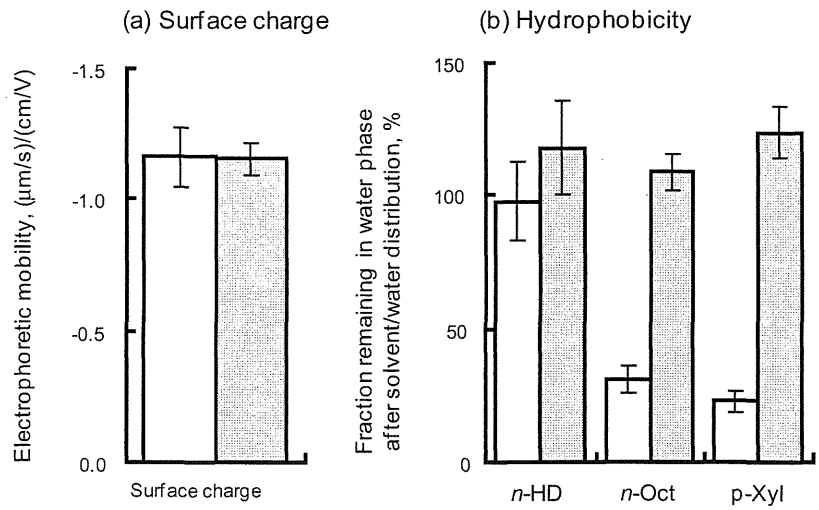

Fig. 6. Comparison of (a) surface charge and (b) hydrophobicity between Qβ and MS2. White and gray columns represent Qβ and MS2, respectively. *n*-HD, *n*-hexadecane; *n*-Oct, *n*-octanol; p-Xyl, p-xylene. Error bars in (a) and (b) indicate SD of 30 and 5 measurements, respectively.

Pore size measurements clearly show that the wood-1 and wood-2 S-PACs had larger pore volume at 20–50 nm than the wood-8 and coconut-2 S-PACs (Table 2); the pore volumes of the high-virus-adsorbable S-PACs were 1.8–2.0 times as much as the averaged pore volume of the low-virus-adsorbable S-PACs. These results agree well with the SEM observations, supporting the hypothesis that the pore size distribution of the S-PACs contributed greatly to virus removal.

3.5. Effect of hydrophobicity of virus on virus removal

The removal of bacteriophage MS2 was ~1 log less than that of Qβ by both wood-1 and wood-2 S-PACs (Table 3). Although the molecular size of an adsorbate controls accessibility to the pores of the activated carbon [26], the diameters of the Qβ and MS2 are almost the same (~23 nm), so this does not explain the difference in removal. Likewise, although the surface charges of viruses depend on the chemistry of their surface proteins, we found no difference in the surface charge between the two viruses (Fig. 6a). Instead, they differed in hydrophobicity (Fig. 6b): MS2 remained in the water phase of all solvent combinations tested, indicating that it has a hydrophilic surface. In contrast, Qβ largely transferred to the solvent phase when *n*-octane and p-xylene were used. This result indicates that the surface of Qβ is more hydrophobic than that of MS2, in agreement with a previous report [27]. Thus, the more hydrophobic the surface of the virus particles is, the greater the virus removal would be expected. As shown in Section 3.3, reducing the surface charge of the activated carbons improved virus removal. The reduction in the surface charge may provide more hydrophobic surface on the carbon apparently, because the reduction allows negatively charged adsorbates to move nearer to the graphite structure on the carbon. Adding to the reduction in the electrophoretic repulsive force, the apparent increase in hydrophobicity of the carbon surface most likely contributed to the high virus removal. Likewise, the hydrophobicity of the viruses contributed to the high removal: the virus having more hydrophobic surface was removed more greatly with the activated carbons.

4. Conclusions

(1) Electrophoretic repulsive force contributed greatly to virus removal: the smaller the repulsion between virus and PAC particles, the greater the virus removal.
(2) The pore size distribution of the PAC contributed greatly to virus removal: PACs with a large volume of pores 20–50 nm in diameter removed virus effectively.
(3) The hydrophobicity of the virus surface contributed greatly to virus removal: the more hydrophobic the surface, the greater the virus removal.
(4) To enhance adsorptive virus removal, activated carbons must have a less negative surface charge and a large volume of pores 20–50 nm wide.

Acknowledgments

Makoto Kobuke and Tomoko Aki made efforts for the experiments on the virus hydrophobicity and the surface functional group of the activated carbons, respectively. This research was supported in part by a Grant-in-Aid for the Encouragement of Young Scientists (2010) from the Ministry of Education, Culture, Sports, Science and Technology of Japan; a Grant-in-Aid (2010) from the Ministry of Health, Labor and Welfare of Japan; and a Kurita Water and Environment Foundation Research Grant (2009).

References

[1] C.P. Gerba, M.D. Sobsey, C. Wallis, J.L. Melnick, Adsorption of poliovirus onto activated carbon in wastewater, Environ. Sci. Technol. 9 (1975) 727–731.
[2] W.A. Hijnen, G.M.H. Suylen, J.A. Bahlman, A. Brouwer-Hanzens, G.J. Medema, GAC adsorption filters as barriers for viruses, bacteria and protozoan (oo)cysts in water treatment, Water Res. 44 (2010) 1224–1234.
[3] P.P. Oza, M. Chaudhuri, Removal of viruses from water by sorption on coal, Water Res. 9 (1973) 707–712.
[4] S.J. Randtke, V.L. Snoeyink, Evaluating GAC adsorptive capacity, J. AWWA 75 (1983) 406–413.
[5] I.N. Najm, V.L. Snoeyink, M.T. Suidan, C.H. Lee, Y. Richard, Effect of particle size and background natural organics on the adsorption efficiency of PAC, J. AWWA 82 (1990) 65–72.
[6] H. Sontheimer, J.C. Crittenden, R.S. Summers, Activated Carbon for Water Treatment, second ed., DVGW-Forschungsstelle, Karlsruhe, Germany, 1988.
[7] Y. Matsui, R. Murase, T. Sanogawa, N. Aoki, S. Mima, T. Inoue, T. Matsushita, Rapid adsorption pretreatment with submicron powdered activated carbon particles before microfiltration, Water Sci. Technol. 51 (6–7) (2005) 249–256.
[8] Y. Matsui, T. Sanogawa, N. Aoki, S. Mima, T. Matsushita, Evaluating submicron-sized activated carbon adsorption for microfiltration pretreatment, Water Sci. Technol.: Water Supply 6 (1) (2006) 149–155.
[9] Y. Matsui, N. Ando, H. Sasaki, T. Matsushita, K. Ohno, Branched pore kinetic model analysis of geosmin adsorption on super-powdered activated carbon, Water Res. 43 (2009) 3095–3103.
[10] N. Shirasaki, T. Matsushita, Y. Matsui, M. Kobuke, K. Ohno, Comparison of removal performance of two surrogates for pathogenic waterborne viruses, bacteriophage Qβ and MS2, in a coagulation–ceramic microfiltration system, J. Membrane Sci. 326 (2009) 564–571.
[11] M.H. Adams, Bacteriophages, Interscience, New York, NY, USA, 1959.
[12] M. Rosenberg, D. Gutnick, E. Rosenberg, Adherence of bacteria to hydrocarbons: a simple method for measuring cell-surface hydrophobicity, FEMS Microbiol. Lett. 9 (1980) 29–33.
[13] N. Shirasaki, T. Matsushita, Y. Matsui, A. Oshiba, K. Ohno, Estimation of norovirus removal performance in a coagulation-rapid sand filtration process by using recombinant norovirus VLPs, Water Res. 44 (2010) 1307–1316.
[14] T. Powell, G.M. Brion, M. Jagtoyen, F. Derbyshire, Investigating the effect of carbon shape on virus adsorption, Environ. Sci. Technol. 34 (2000) 2779–2783.
[15] S.L. Penrod, T.M. Olson, S.B. Grant, Whole particle microelectrophoresis for small viruses, J. Colloid Interface Sci. 173 (1995) 521–523.
[16] J.A. Redman, S.B. Grant, T.M. Olson, J.M. Adkins, J.L. Jackson, M.S. Castillo, W.A. Yanko, Physicochemical mechanisms responsible for the filtration and mobilization of a filamentous bacteriophage in quartz sand, Water Res. 33 (1999) 43–52.
[17] B. Yuan, M. Pham, T.H. Nguyen, Deposition kinetics of bacteriophage MS2 on a silica surface coated with natural organic matter in a radial stagnation point flow cell, Environ. Sci. Technol. 42 (2008) 7628–7633.
[18] S.E. Mylon, C.I. Rinciog, N. Schmidt, L. Gutierrez, G.C.L. Wong, T.H. Nguyen, Influence of salts and natural organic matter on the stability of bacteriophage MS2, Langmuir 26 (2010) 1035–1042.
[19] J. Gregory, Particles in Water: Properties and Processes, CRC Press, Boca Raton, FL, USA, 2006.
[20] J.C. Lance, C.P. Gerba, Effect of ionic composition of suspending solution on virus adsorption by a soil column, Appl. Environ. Microbiol. 47 (1984) 484–488.
[21] D.G. Jewett, T.A. Hilbert, B.E. Logan, R.G. Arnold, R.C. Bales, Bacterial transport in laboratory columns and filters: influence of ionic strength and pH on collision efficiency, Water Res. 29 (1995) 1673–1680.
[22] H. Cao, F.T.C. Tsai, K.A. Rusch, Impact of salinity on MS-2 sorption in saturated sand columns–fate and transport modeling, J. Environ. Eng. 135 (2009) 1041–1050.
[23] J. Zhuang, Y. Jin, Virus retention and transport through Al-oxide coated sand columns: effects of ionic strength and composition, J. Contaminant Hydrol. 60 (2003) 193–209.
[24] M. Pham, E.A. Mintz, T.H. Nguyen, Deposition kinetics of bacteriophage MS2 to natural organic matter: role of divalent cations, J. Colloid Interface Sci. 338 (2009) 1–9.
[25] R.J. Martin, Activated carbon product selection for water and wastewater treatment, Ind. Eng. Chem. Prod. Res. Dev. 19 (1980) 435–441.
[26] C. Moreno-Castilla, Adsorption of organic molecules from aqueous solutions on carbon materials, Carbon 42 (2004) 83–94.
[27] J. Langlet, F. Gaboriaud, J.F.L. Duval, C. Gantzer, Aggregation and surface properties of F-specific RNA phages: implication for membrane filtration processes, Water Res. 42 (2008) 2769–2777.
[28] H.P. Boehm, Some aspects of the surface-chemistry of carbon-blacks and other carbons, Carbon 32 (1994) 759–769.
[29] H.P. Boehm, Surface oxides on carbon and their analysis: a critical assessment, Carbon 40 (2002) 145–149.

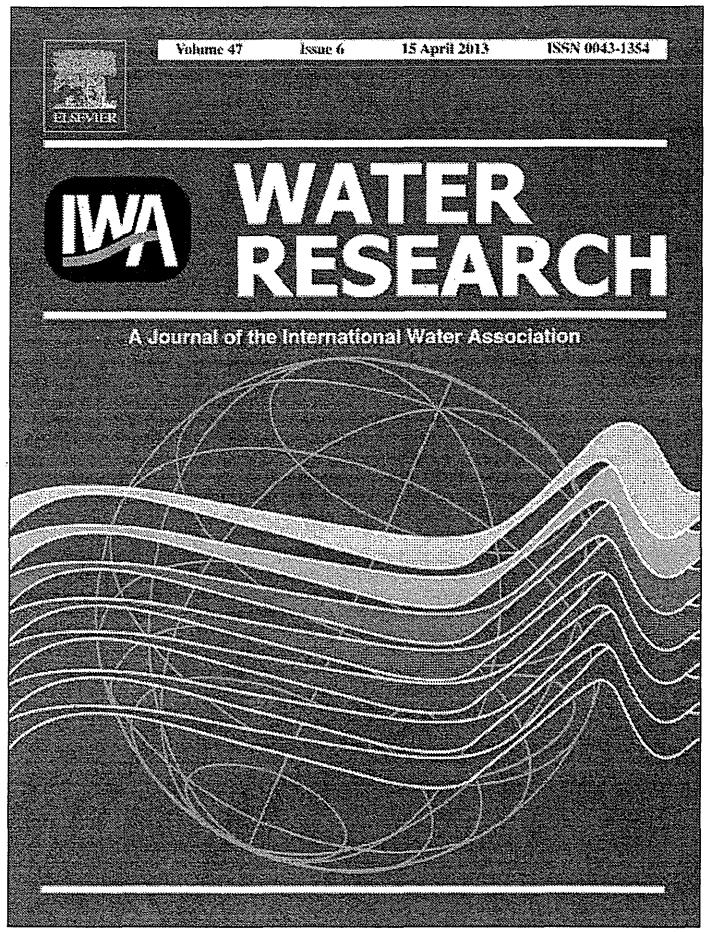

WATER RESEARCH 47 (2013) 2075–2084

Available online at www.sciencedirect.com

SciVerse ScienceDirect

journal homepage: www.elsevier.com/locate/watres

Minimizing residual aluminum concentration in treated water by tailoring properties of polyaluminum coagulants

Masaoki Kimura [a], *Yoshihiko Matsui* [b,*], *Kenta Kondo* [a], *Tairyo B. Ishikawa* [a], *Taku Matsushita* [b], *Nobutaka Shirasaki* [b]

[a] *Graduate School of Engineering, Hokkaido University, N13W8, Sapporo 060-8628, Japan*
[b] *Faculty of Engineering, Hokkaido University, N13W8, Sapporo 060-8628, Japan*

ARTICLE INFO

Article history:
Received 13 August 2012
Received in revised form
2 November 2012
Accepted 21 January 2013
Available online 31 January 2013

Keywords:
Basicity
PACl
Sulfate
Monomer Al
Coagulation

ABSTRACT

Aluminum coagulants are widely used in water treatment plants to remove turbidity and dissolved substances. However, because high aluminum concentrations in treated water are associated with increased turbidity and because aluminum exerts undeniable human health effects, its concentration should be controlled in water treatment plants, especially in plants that use aluminum coagulants. In this study, the effect of polyaluminum chloride (PACl) coagulant characteristics on dissolved residual aluminum concentrations after coagulation and filtration was investigated. The dissolved residual aluminum concentrations at a given coagulation pH differed among the PACls tested. Very-high-basicity PACl yielded low dissolved residual aluminum concentrations and higher natural organic matter (NOM) removal. The low residual aluminum concentrations were related to the low content of monomeric aluminum (Ala) in the PACl. Polymeric (Alb)/colloidal (Alc) ratio in PACl did not greatly influence residual aluminum concentration. The presence of sulfate in PACl contributed to lower residual aluminum concentration only when coagulation was performed at around pH 6.5 or lower. At a wide pH range (6.5–8.5), residual aluminum concentrations <0.02 mg/L were attained by tailoring PACl properties (Ala percentage ≤0.5%, basicity ≥85%). The dissolved residual aluminum concentrations did not increase with increasing the dosage of high-basicity PACl, but did increase with increasing the dosage of normal-basicity PACl. We inferred that increasing the basicity of PACl afforded lower dissolved residual aluminum concentrations partly because the high-basicity PACls could have a small percentage of Ala, which tends to form soluble aluminum–NOM complexes with molecular weights of 100 kDa–0.45 μm.

1. Introduction

Alum and polyaluminum chloride (PACl) coagulants are widely used at water treatment plants to remove turbidity and dissolved substances from water. However, concerns have been raised that the use of such coagulants may increase aluminum concentrations in treated water (Miller et al., 1984; Ohno et al., 2009). High aluminum concentrations in treated water are associated with several problems, including increased turbidity due to the formation of aluminum precipitates. Also of concern are human health hazards (Flaten, 2001; World Health Organization, 2004; Gupta et al., 2005).

The concentration of residual aluminum remaining in water treated with aluminum coagulants is influenced by

* *Corresponding author.* Tel./fax: +81 11 706 7280.
E-mail address: matsui@eng.hokudai.ac.jp (Y. Matsui).
0043-1354/$ – see front matter © 2013 Elsevier Ltd. All rights reserved.
http://dx.doi.org/10.1016/j.watres.2013.01.037

many factors. Among these, control of solution pH is key to minimizing the aluminum concentration (Licsko and Szakal, 1988; Van Benschoten and Edzwald, 1990; Van Benschoten et al., 1994; Driscoll and Letterman, 1995). The use of aluminum coagulants at around pH 6.5 is one approach for minimizing residual aluminum concentrations. Although residual aluminum concentrations can be controlled by adjusting pH to slightly acidic values, this strategy is not widely practiced, because it requires a pH increase post-treatment to control corrosion in water distribution networks. In addition, small water treatment facilities still experience difficulties in attaining this pH optimization, because the small size of the plant provides little buffering for fluctuation in operation. Moreover, such small facilities often have limited resources and limited access to the expertise needed to control acid/base addition and to optimize pH conditions. In Japan, the drinking water quality guideline for aluminum is 0.1 mg/L, but water treatment plants usually set stricter values for finished water, e.g., <0.05 mg/L. However, meeting such values is often difficult, particularly when the pH of raw water is high due to algae growth. Under such alkaline conditions, high concentrations of residual aluminum often remain following water treatment. Therefore, the development of coagulants that can easily decrease residual aluminum concentrations to <0.05 mg/L, even for treated water in which coagulation pH is not optimized, is highly desired.

Residual aluminum concentrations after water treatment can also vary with coagulants (alum and PACls). For example, Jekel (1991) conducted jar tests with alum and four commercial prehydrolyzed aluminum salts and reported that, at pH values of >7.5, the use of two of the four prehydrolyzed products resulted in lower residual aluminum concentrations than did the use of alum. Simpson et al. (1988) suggested the use of PACl instead of alum as an approach for reducing residual aluminum concentrations. Yan et al. (2008a) reported that the dissolved residual aluminum concentrations for high-basicity (basicity = OH/Al = 2.0 or OH/(Al × 3) × 100 = 67%) PACl at acidic and basic pH (<5.5 and >7.5) were lower than that for medium-basicity PACl and $AlCl_3$. However, at neutral pH (7.0), dissolved residual aluminum concentrations were the same for $AlCl_3$ and the PACls. These investigators attributed the lower aluminum concentrations to the low content of monomeric aluminum species in the high-basicity PACl (Yan et al., 2007). However, a low residual aluminum concentration (<0.1 mg/L) was not attained at any pH for any coagulants with basicities 0–2.5. In practice, controlling residual aluminum concentration to <0.1 mg/L is difficult, in particular when PACls are used at pH > 7.5 (Matsukawa et al., 2006). Very recently, Yang et al. (2011) reported that residual aluminum concentrations varied in the following order: PACl of basicity 1.5 > 2.3 ≥ 2.0. However, the comparison, which was made on different coagulation pH values because pH after dosing coagulants depressed differently depending on coagulant basicity, might be imprecise. Overall the previous results suggest that the residual aluminum concentration could be controllable by adjusting PACl properties, but the specific PACl properties for lowering residual aluminum concentrations <0.05 mg/L have yet to be investigated. It should also be noted that most of the previous studies used non-sulfated PACls, although sulfated PACls are widely applied in practice because sulfate enhances the flocculation performance of PACls. However, inclusion of sulfate ions in high-basicity PACls with high aluminum content limits the PACls' long-term chemical stability, so the basicity of practically applied PACls with Al content >5% (w/w) is typically limited to 2.0 to allow storage of the compounds for >6 months.

In this study, we evaluated the efficacy of PACls, including those with an extremely high basicity of 2.7, in terms of residual aluminum concentration at neutral and alkaline pH.

2. Materials and methods

2.1. Coagulants

Five aluminum-based coagulants were evaluated in the first set of experiments (Table 1S, Supplementary Information). Commercially available PACls with standard basicities of 1.8 and 1.5 (designated PACl-61s and PACl-51s, respectively. The numbers, "51" and "61", in the names indicate percent basicity values. "s" indicates "sulfated".) were provided by Taki Chemical Co. (Kakogawa, Japan). PACl-71s is a trial coagulant product (presently commercially available) provided by the same company. These PACls were produced by dissolving $Al(OH)_3$ solids in hydrochloric and sulfuric acid (as described by, e.g., Itoh and Sato, 1995; Sato and Matsuda, 2009). Alum was provided as a solution (Taki Chemical Co.). The PACls and alum were used in jar tests immediately after dilution with Milli-Q water. $AlCl_3$ solution was prepared by dissolving reagent-grade $AlCl_3 \cdot 6H_2O$ (Wako Pure Chemical Industries, Osaka, Japan) in Milli-Q water (Milli-Q Advantage, Nihon Millipore, Tokyo, Japan); this solution was considered as a reference PACl with a basicity of zero (Yan et al., 2008a).

After the experiments using the five coagulants described above were completed, we conducted the second set of experiments by using 12 additional coagulants. Four PACls out of 12 were prepared by a base titration method in the authors' laboratory (Shen and Dempsey, 1998; Yan et al., 2008b). PACl-72b and PACl-90by ("b" in the name indicates high Alb percentage relative to other PACls of the same basicity. "x", "y", and "z", some of which appear later, have no special meaning.) was prepared with the following procedure. NaOH (0.3 M) was titrated to a 500-mL Erlenmeyer flask containing an 80 mL of $AlCl_3$ solution (0.5 M) by a peristaltic pump at rate of 4 mL/min to bring the target basicity. During the titration the solution in the flask was agitated and the temperature was kept at 85–90 °C by a combined hot-plate magnetic-stirrer device. PACl-90bx was prepared from 0.6 M NaOH and 1.0 M $AlCl_3$ solutions by the same method. For PACl-72c ("c" in the name indicates high Alc percentage), after titrating 0.9 M NaOH into 1.5 M $AlCl_3$ solution, the solution was kept at 85–90 °C for 12 h. PACl-50, PACl-61, and PACl-70 were trial coagulant products (Taki Chemical Co.) produced from NaOH and $AlCl_3$. PACl-85x, y, and z and PACl-90x and y were also trial coagulant products that produced from commercial aluminum chlorohydrate solution (Al_2O_3 23%, sulfate ion 0%, relative density of 1.3, Taki Chemical Co.) and soda ash.

The distributions of aluminum species in the coagulants were analyzed by the ferron method. On the basis of their

reaction rates with ferron reagent (8-hydroxy-7-iodo-5-quinoline sulfonic acid, Wako Pure Chemical Industries), the aluminum species were divided into three categories: Ala, Alb, and Alc. Ala denotes aluminum species that reacted with ferron instantaneously (within 30 s). Alb denotes species that reacted within 120 min. Alc denotes species that did not react. These species were assumed to be monomeric, polymeric, and colloidal aluminum species, respectively (Wang et al., 2004). Ferron analyses of the coagulants were conducted immediately (1–2 min) after diluting coagulants with Milli-Q water to 2.7 g-Al/L (Wang et al., 2004; Jia et al., 2004). Dilution reportedly has little effect on the ferron speciation distribution of PACl (Wang et al., 2004), and we also observed a negligible effect of dilution on ferron speciation distribution in the present study (data not shown). After adding the ferron reagent into diluted coagulant, the mixture was immediately shaken, and then the absorbance at 366 nm in an 1-cm or 5-cm cell was measured by using at the predetermined times.

Using membranes with various molecular weight cutoffs (MWCOs), we also investigated the MW distributions of aluminum species in the coagulants. Coagulants containing 2.7 g-Al/L (the same concentration as that used for the ferron method) were filtered through ultrafiltration (UF) membranes with nominal MWCOs of 500 Da (cellulose acetate membrane, Amicon YC, Nihon Millipore) and 3 kDa (regenerated cellulose membrane, Ultracell PL, Nihon Millipore) in a 50-mL stirred cell (Amicon 8050 series, Nihon Millipore) under 0.5 MPa pressure immediately after preparation of the solution. Filtration was performed until 2 mL was collected from a 50-mL sample. Aluminum concentrations were analyzed with an inductively coupled plasma mass spectrometer (ICPMS, HP-4500 and HP-7700, Agilent Technologies, Inc.).

2.2. *Jar tests*

Jar tests were performed with a jar test apparatus at room temperature (~20 °C) unless otherwise noted. Raw water (Table 1) was transferred to a 1-L square plastic beaker. After a predetermined volume of HCl (0.1 N) or NaOH (0.1 N) was added to bring the final coagulation pH to a target value, a coagulant was injected into the raw water sample. The mixture was stirred rapidly for 1 min ($G = 200\ s^{-1}$, 136 rpm) and then slowly for 10 min ($G = 20\ s^{-1}$, 30 rpm). The mixture was then left to rest for 1 h so that the aluminum floc particles generated would settle. Then samples were taken from the beaker and filtered through a 0.45-μm polytetrafluoroethylene (PTFE) membrane filter (DISMIC-25HP; Toyo Roshi Kaisha, Ltd., Tokyo) unless otherwise noted for quantification of the dissolved organic carbon (DOC; Sievers 900 TOC Analyzer, GE Analytical Instruments, Boulder, Colorado, USA) and aluminum. The coagulation pH and turbidity were measured after settling. Decreases in turbidity were high in most of the experiments because the coagulant dosages were sufficient for formation of floc particles. Therefore, coagulant performance was evaluated mainly in terms of DOC removal. For the first set of experiments, we investigated the size distribution of the residual aluminum particles by using membranes with nominal MWCOs of 100 k, 3 k, and 500 Da, as well as 0.45-μm pore size. Jar tests were performed at a constant dosage with varying pH. The data at a fixed pH value were obtained by interpolation because final coagulation pH hardly coincided with the target value, e.g., the interpolation of the results for two pH ranges (pH 7.2–7.4 and 7.6–7.8) surrounding the target pH value of 7.5.

3. Results and discussion

3.1. *Coagulant properties*

The percentages of aluminum species in the coagulants, as determined by means of the ferron method, are shown in Fig. 1A and C. Aluminum species distributions were very different depending on basicity and production methods. Among the PACls, Alc percentage generally increased with increasing basicity. The inclusion of sulfate in the PACls did not largely influence aluminum species distribution (compare PACl-50 and -51s, PACl-61 and -61s and PACl-70 and -72s in Fig. 1C). The aluminum speciations of PACl-51s (basicity 1.5) was similar to the speciation observed for another Japanese commercial PACl (basicity 1.4) analyzed by Lin et al. (2008). Most of the PACls, except some laboratory-prepared PACls (PACl-72b, -90bx, and -90by), contained small amounts of Alb, which is typically observed for commercial PACl products (Wang and Hsu, 1994; Chen et al., 2006).

MW distributions of aluminum species were determined for PACl-71s, -61s, and -51s, and for $AlCl_3$ and alum. PACl-71s had the highest percentage of aluminum in the high-MW fraction (>3 kDa), followed by -61s, -51s, alum, and $AlCl_3$, in that order (Fig. 1B). The results from the ferron method and the MW distribution analysis strongly agree in indicating that, of the tested coagulants, PACl-71s contained the smallest amount of monomeric aluminum (low MW) and the largest amount of colloidal aluminum (high MW).

Table 1 – Characteristics of raw water samples used in this study.

Designation	pH	Turbidity (NTU)	Alkalinity (mg/L as $CaCO_3$)	DOC (mg/L)	UV_{260} (cm^{-1})	Source	Sampling date
Toyohira River A	7.7	1.4	40	1.0	0.033	Toyohira River, Hokkaido, Japan	26 September 2008
Toyohira River B	7.5	0.96	21	1.0	0.031	Toyohira River, Hokkaido, Japan	8 July 2009
Toyohira River C	7.4	9.0	17	1.0	0.031	Toyohira River, Hokkaido, Japan	24 June 2011
Chibaberi River A	7.7	4.9	105	4.0	0.25	Chibaberi River, Hokkaido, Japan	13 August 2008
Chibaberi River B	7.4	2.4	31	2.1	0.10	Chibaberi River, Hokkaido, Japan	13 November 2009
Wani River	7.6	5.4	80	3.2	0.065	Wani River, Ibaraki, Japan	26 December 2011